Research Journal of Applied Sciences, Engineering and Technology 6(6): 1059-1064, 2013
ISSN: 2040-7459; e-ISSN: 2040-7467

Submitted: October 31, 2012 Accepted: December 21, 2012 Published: June 30, 2013

Fluid Dynamics Characteristics during Stall Inception Process in a Centrifugal Fan

Lei Zhang, Qian Zhang and Chenxing Hu
Key Laboratory of Condition Monitoring and Control for Power Plant Equipment of Ministry of Education, North China Electric Power University, Hebei, Baoding 071003, China

Abstract: Based on the three-dimensional elliptic governing equations and the throttle model, an unsteady numerical simulation of rotating stall is undertaken in the case of G4-73 type centrifugal fan and the correctness of simulation results is verified by experiments. In this study a new rotating stall inception criterion is put forward, that the inlet flow or outlet back pressure fluctuations gradually increase in the value range. Numerical results show that the stall inception comes in obvious modal waveform, which belongs to the suction side stall caused by the incident angle changes due to the decrease of the flow. The relative velocity distribution of the impeller at different times indicates that the first bottleneck area occurs in the impeller channel near the volute tongue, while the other flow passages get improved and the flow field is unevenly distributed along the circumferential direction.

Keywords: Centrifugal fan, numerical, stall inception, simulation, volute tongue

INTRODUCTION

Rotating stall is a kind of internal unsteady flow phenomenon in the fan. Because the rotating stall boundary line is close to the maximum efficiency curve in the centrifugal fan (Hou *et al*., 2003). It's likely to cause the fan to enter the stall area deviating from the design conditions, which may induce the fatigue and fracture problems at heavily stressed points of blades. Without effective containment, rotating stall may lead to surge, causing vibration of the fan body and connecting pipes, moreover, leading to accidents. In order to realize the active control of rotating stall, it is necessary to find the most favorable location and time to introduce the reversed-phase perturbation and the key is to analyze the characteristics and mechanism of stall inception based on the unsteady three-dimensional fluid dynamics characteristics of the fan.

Studies on the internal flow field distribution under the condition of rotating stall are mainly divided into experiments and numerical simulation and experimental measurement has been the primary means since 1960s. Lennemann (1970) discussed the reasons for the formation of stall cells under the condition of low flow rate with the method of hydrogen bubble flow visualization. Rodgers (1978) experimentally studied the stall in the centrifugal compressor with a vane less diffuser and found that improving the diffuser factors can increase the stall margin. Vlad *et al*. (2011) examined the impact of gas blowing technology on the flow field of centrifugal pump under the state of rotating stall.

With the development of computer technology and numerical methods, since the late 1980s, some scholars have used the numerical stall algorithm, namely three-dimensional non-steady Reynolds averaged N-S equation, to directly calculate the whole stall process as reported by Takayuki *et al*. (2011). Masaki and Kaji (2009) found that the interactions between the tip clearance vortex at the top of shock wave has an important influence on the loss of steady flow through a single-channel three-dimensional unsteady simulation on transonic compressor rotor at near stall conditions. Guo *et al*. (2009) undertook a numerical simulation on rotating stall phenomenon of high-speed centrifugal compressor with a vane less diffuser by using a gas chamber model. Wu *et al*. (2011) and Li *et al*. (2011) also had obtained remarkable achievements on axial flow compressor rotating stall phenomena.

In summary, the present studies on the flow field characteristics during the evolution of the stall inception mainly concentrate on the axial compressor. The mechanism and evolution characteristics of rotating stall have differences between centrifugal fan and compressor due to the differences in geometric characteristics and performance continuity. Thus in order to reveal the mechanism of stall inception, the G4-73 centrifugal fan rotating stall is numerical simulated based on the throttle model with the parallel computing platform and both the manifestations and fluid dynamics characteristics of stall inception are analyzed in this study.

COMPUTATIONAL MODEL

Geometric model and meshing: The configuration studied is a G4-73No.8D type centrifugal fan at rotational speed of 1450 rpm and with an inlet diameter

Corresponding Author: Lei Zhang, Key Laboratory of Condition Monitoring and Control for Power Plant Equipment of Ministry of Education North China Electric Power University, Hebei, Baoding 071003, China

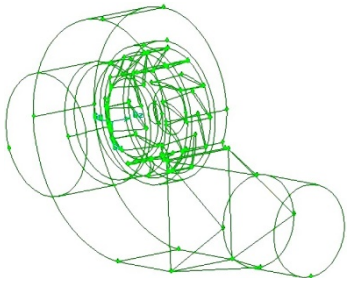

Fig. 1: Geometric model of centrifugal fan

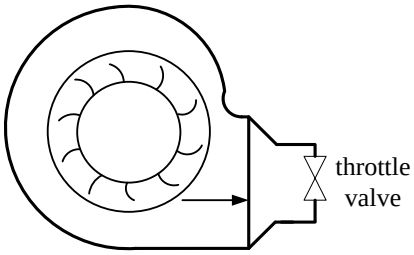

Fig. 2: Throttle valve model

of 0.568 m, an outlet diameter of 0.8 m and blade number is 12. The calculation areas of flow field include five domains: inlet pipe, current collector, impeller, and volute and outlet pipe. The three-dimensional geometric model of the centrifugal fan can be built with GAMBIT as shown in Fig. 1. For inlet pipe, current collector and outlet pipe, a hexahedral structured grid is generated. For impeller and volute, which contain more complex flow field, a tetrahedral unstructured grid with better applicability is generated. A boundary layer and size function are adopted in the blades and volute tongue region to density grid and the total amount of grid is 3,008,800.

Throttle valve model: In order to simulate the phenomenon of rotating stall, a centrifugal fan stall model is established as shown in Fig. 2. The operating condition of the ventilation system is determined by the intersection of the fan performance curve and valve throttling line, which is directly connected in structure. The operating point changes with the throttle opening and the slope of performance curve and throttle line differs at the same operating point, thus the stability analysis can be conducted. Given the incompressible homogeneous fluid in the fan, the throttle function can be expressed as:

$$Ps_{out}(t) = Pi_{in} + \frac{1}{2}\frac{k_0}{k_1}\rho U^2 \quad (1)$$

where,

Ps_{out} = The outlet back pressure

Pi_{in} = The atmospheric pressure

k_0 = A constant

k_1 = The valve opening

ρ = The air density

U = The outlet axial velocity

The valve opening k_1 which is supposed to set the throttle initial operating conditions can be set to 1 by setting k_0. The occurrence of rotating stall can be gradually achieved with k_1 decreasing, which leads to the decreasing of flow, until the valve is completely shut.

Governing equations: A non-steady Reynolds time-averaged Navier-Stokes equations (URANS) is adopted to accurately describe the motion law in the centrifugal fan since the flow field is non-steady under the condition of rotating stall. The governing equations include the continuity equation, Navier-Stokes equations and Realizable k-ε turbulence model:

$$\frac{\partial \upsilon_i}{\partial x_i} = 0 \quad (2)$$

$$\rho\frac{\partial \upsilon_i}{\partial t} + \rho\frac{\partial}{\partial x_j}(\upsilon_i\upsilon_j) = -\frac{\partial P}{\partial x_i} + \frac{\partial}{\partial x_j}\left(\mu\frac{\partial \upsilon_i}{\partial x_j} - \rho\overline{u_i u_j}\right) + \rho f_i \quad (3)$$

$$\frac{\partial}{\partial t}(\rho k) + \frac{\partial}{\partial x_i}(\rho k u_i) = \frac{\partial}{\partial x_i}[(\mu + \frac{\mu t}{\sigma_k})\cdot\frac{\partial k}{\partial x_j}] + G_k + G_b - \rho\varepsilon - Y_M + S_k \quad (4)$$

$$\frac{\partial}{\partial t}(\rho\varepsilon) + \frac{\partial}{\partial x_j}(\rho\varepsilon u_j) = \frac{\partial}{\partial x_j}[(\mu + \frac{\mu t}{\sigma_\varepsilon})\cdot\frac{\partial k}{\partial x_j}] + \rho C_1\cdot S_\varepsilon - \rho C_2\cdot\frac{\varepsilon^2}{k+\sqrt{\nu\varepsilon}} + C_{1\varepsilon}\cdot\frac{\varepsilon}{k}\cdot C_{3\varepsilon}\cdot G_b + S_\varepsilon \quad (5)$$

Discrete control equations of the finite volume method are adopted and the semi- implicit method of concerted pressure coupled equations is used to account for pressure-velocity coupling. A second-order upwind difference scheme and a central difference scheme are adopted to discretize relatively convection and diffusion terms. An implicit scheme is used to describe unsteady simulation time discretization and time accuracy is second order.

Boundary conditions: At the inlet, the boundary condition is a purely axial injection condition and the total pressure is 1atm. Pressure outlet boundary condition and static pressure, which is obtained through steady simulation, are set to outlet. The throttle model is considered for unsteady simulation and the user-defined function (1) is used to achieve each time step of iterative calculation.

The physical time step of unsteady calculation is 0.0001725s (equivalent to 20 time steps set in an

impeller). The no-slip boundary condition is adopted for wall. The Multiple Reference Frame (MRF) model is used to account for parameter transfer between rotation region and static region in steady calculation, while moving mesh model is used in unsteady calculation.

SIMULATION RESULTS AND DISCUSSION

To avoid the affect on calculation accuracy from grid number, four conditions are selected to conduct grid independence computing corresponding to the grid number of 16×10^5, 24×10^5, 30×10^5 and 38×10^5. Comparisons between performance curve corresponding to different grid number calculated and experimental performance curve is illustrated in Fig. 3. As shown in the figure, the gap between the numerical results and the experimental results tends to be smaller. Giving full consideration to the calculation accuracy and computation time, the grid number 30×10^5 is selected here for simulation. The calculation results agree well with the experimental results. The error is within 3% and the error near the maximum efficiency point is within 1%.

Generally, there are mainly two ways to judge the rotating stall in turbomachines: one alternative is to layout circumferential uniform monitoring points near the blade inlet to monitor relative rate; another is to observe whether the circumferential distribution occurs in internal flow field and spreads circumferentially.

Figure 4 shows the flow curves when valve opening is relatively 0.9 and 0.89. It can be seen from the figure that a stable and convergent result can be progressive approached along the throttle line without the occurrence of rotating stall when the valve opening is 0.9. A convergent solution seems to be obtained for a period of time when the valve opening becomes 0.89, but the fan gradually enters stall condition as the fluctuations of inlet flow and outlet pressure increasing. Stall inception gradually develops into stable stall cells and the fan maintains in a new periodic steady operating condition. Given the analysis above, it can be treated as a criterion of the rotating stall when the fluctuation range of inlet flow or outlet pressure gradually expands in the process of calculation.

The axial section of the centrifugal fan when Z = 34.44 is shown in Fig. 5 and the point A near the blade leading edge, where the relative velocity of is monitored, is marked. To facilitate the analysis, the relative position of the impeller and the volute tongue mentioned below corresponds to this figure. Figure 6 shows the variation curve of the relative velocity at point A. It can be seen that the stall inception presents a significant modal waveform and it takes 50 rotor cycles for stall inception to develop into stall cells, showing a progressive growth in this transition process.

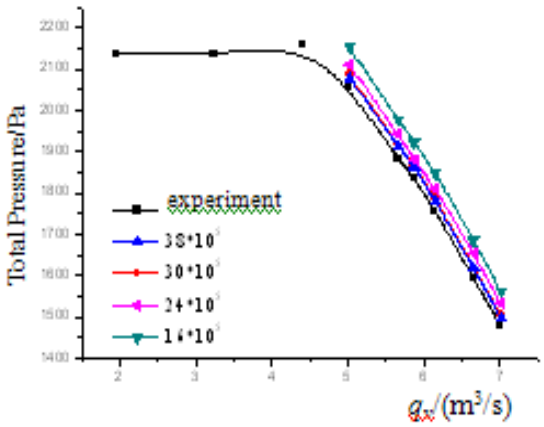

Fig. 3: Relation of full pressure and flowrate

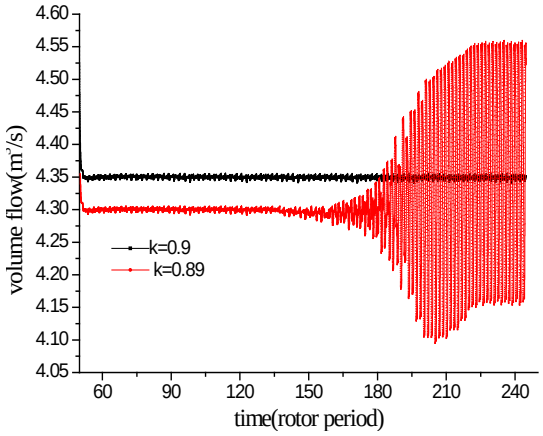

Fig. 4: Flowrate variations with time on two valve opening

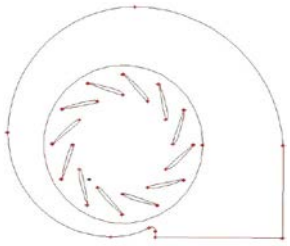

Fig. 5: Monitoring point distribution

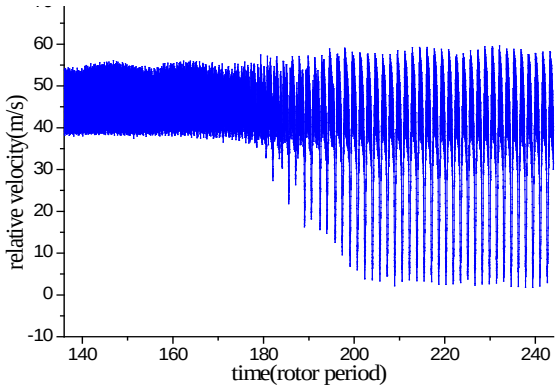

Fig. 6: Relative speed variation with time

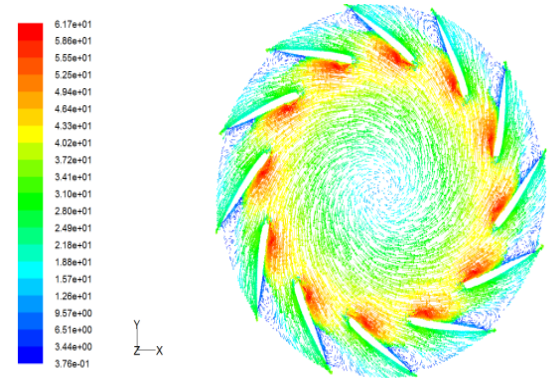

a) Z = 30

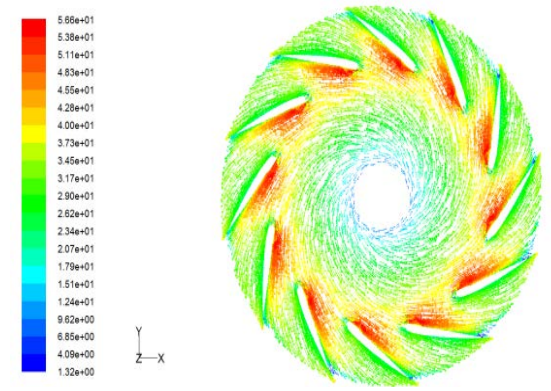

b) Z = 38.5

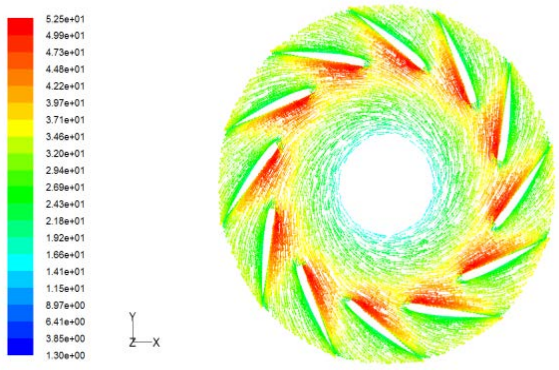

c) Z = 46

Fig. 7: Vectors of relative speed at different axial cross sections when k_1=2

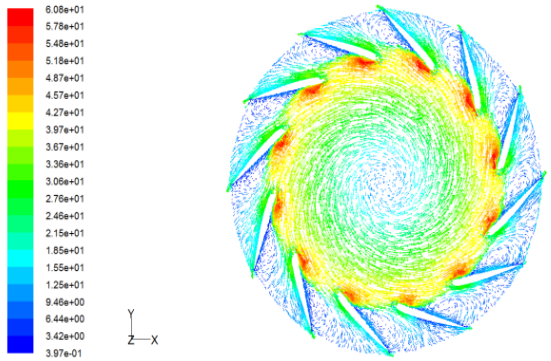

a) Z = 30

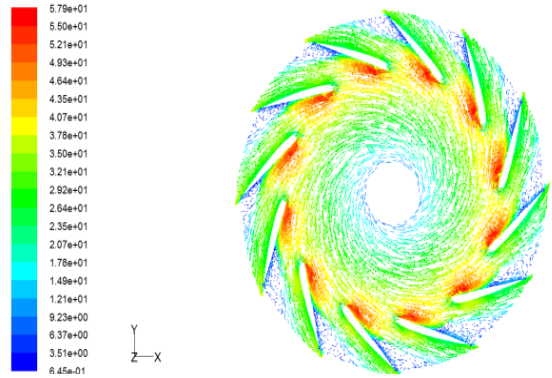

b) Z = 38.5

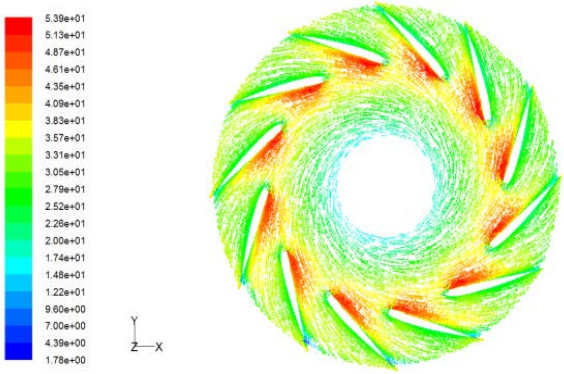

c) Z = 46

Fig. 8: Vectors of relative speed at different axial cross sections when k_1= 0.89(The 137th rotational period)

In order to figure out the mechanism of the stall inception, three kinds of impeller axial section are selected to illustrate relative velocity field. Z = 30, Z = 38.5 and Z = 46 cross-sections are separately close to the shrouded surface, a half of blade height and the hub surface. The rotation cycle is relatively 137 and 170 with the valve opening is 2 or 0.89.

The relative velocity vector of different axial section when the valve opening is 2 is shown in Fig. 7. It can be seen from the figure that relative velocity along the circumferential direction is uneven in distribution with obvious jet-wake structure when the fan is near design condition. Positive incidence angle in circumferential periodic distribution and radial countercurrent area caused by boundary layer separation occur in the flow passage with the separated vortex occupies 1/5 of the flow area when Z = 30. A very small boundary layer separation region appears when Z = 38.5, whereas the incidence angle is almost zero and no boundary layer separation occur in the flow channel when Z = 46. This is because the airflow close to the front plate and the impeller inlet boundary suddenly turns from axial into radial when Z = 38.5, making the relative velocity near the front disc

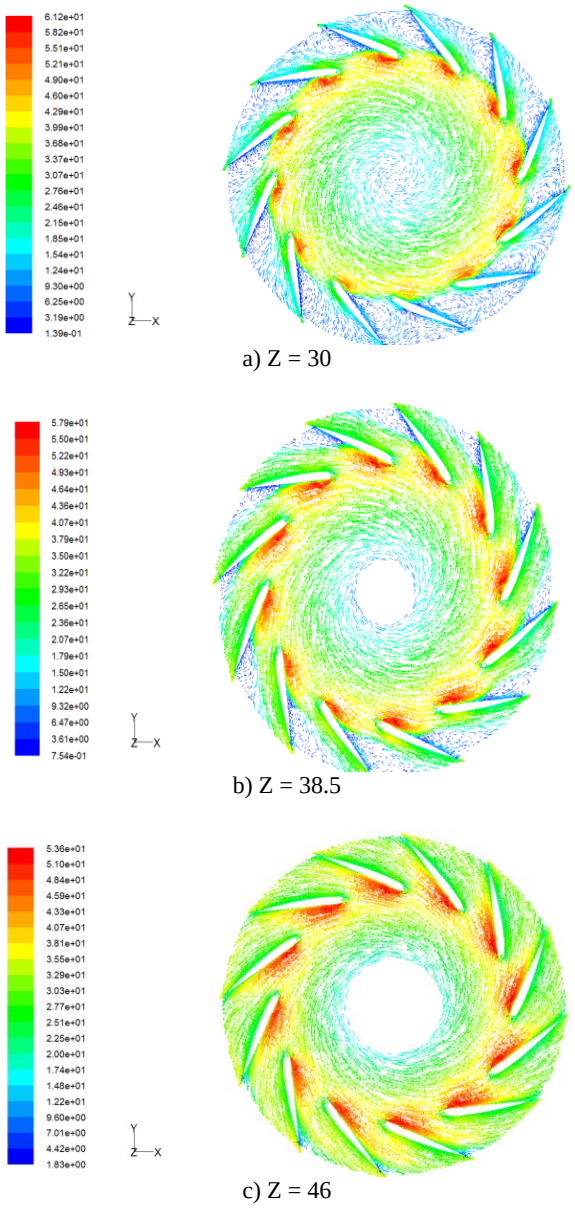

Fig. 9: Vectors of relative speed at different axial cross sections when *k*1=0.89(The 170th rotational period)

decrease, which leads to inlet angle and boundary layer separation in suction side.

Figure 8 illustrates the relative velocity vector distribution of different axial section at 137th rotating cycle when k_1 = 0.89. It can be seen that the area occupied by the separated vortex caused by boundary layer separation at Z = 30 section increases with the flow rate decreasing. The separated vortex near the volute tongue is the largest, but not large enough to block the channel and lead to rotating stall. Boundary layer separation also appears at Z = 38.5 sections and the separated vortex occupies 1/3 of the flow area. Small boundary layer separation region appears near the volute tongue at Z = 46 section. Meanwhile, the influence of the volute tongue on the internal flow of impeller tends to be greater.

Figure 9 illustrates the relative velocity vector distribution of different axial section at 170th rotating cycle when k_1 = 0.89.With the affect of volute tongue, the separation area further increases in the two impeller channels near the volute tongue at Z = 30 section and it almost blocks the entire flow channel with the area occupied by separation vortex in other flow channels decreasing in different level. The separation area in the flow channel near volute tongue increases at the Z = 38.5 section, but not large enough to block the entire flow channel. Separation area slightly larger than that of the 137th rotation cycle occurs in the flow channel near volute tongue at the Z = 38.5 section. Meanwhile, stall inception occurs at the section near the front disc, but has not yet developed into circumferential rotating stall cells.

Based on the analysis above, the rotating stall studied here is caused by the incident angle generated by flow decreasing at the suction side. Under design conditions, boundary layer separation occurs at the blade suction side near the front disc. With the throttle valve opening gradually turned down, the blade inlet angle increases and the separation vortex gradually occupies a larger area of the flow channel. When it comes to a critical opening, separation vortex area persistently increases in the flow channel near volute tongue until stall inception due to the volute tongue, while the separation vortex areas in other flow channels decrease and the flow field is improved with uneven circumferential distribution. For that reason, volute tongue is of great importance on the generation of rotating stall inception.

CONCLUSION

In this study, based on the Realizable k - ε turbulence model and throttle valve function, rotating stall in a centrifugal fan has been numerical simulated and the conclusions have been drawn as follows:

- The correctness of the simulation results is verified through the grid independence computing and centrifugal fan performance test. Stall inception presents obvious modal waveform and develops into a stall cell after 50 rotor cycles
- A new rotating stall inception criterion is put forward in this study, namely rotating stall inception occurs when the fluctuation range of inlet flow or outlet pressure gradually expands in the process of calculation through monitoring
- Volute tongue is of great importance on the generation of rotating stall inception. When it comes to a critical opening, separation vortex area persistently increases in the flow channel near volute tongue until stall inception due to the volute

tongue, while the separation vortex areas in other flow channels decrease and the flow field is improved with uneven circumferential distribution.

ACKNOWLEDGMENT

This study was supported by The Fundamental Research Funds for the Central Universities (12QN39) and National Natural Science Foundation of Hebei Province (E2012502016).

REFERENCES

Guo, Q., X.C. Zhu and Z.H. Du, 2009. Numerical simulation of rotating stall inside high speed centrifugal compressor using entire geometry mesh. J. Mech. Eng., 45(6): 284-289.

Hou, J.H., S.L. Wang and L.S. An, 2003. Characteristic analysis on rotating stall of centrifugal fan based on a family of reformed harmonic wavelet. Power Eng., 23(6): 2814-2818.

Lennemann, E., 1970. Unsteady flow phenomenon in rotating centrifugal impeller passages. J. Eng. Power, 92(1): 65-72.

Li, Q.P., Y.H. Wu, W.L. Chu and H.G. Zhang, 2011. Full-annulus simulations on axial compressor rotor at near stall condition. J. Aerosp. Power, 26(10): 2330-2338.

Masaki, D. and S. Kaji, 1997. Numerical analysis of transonic compressor rotor flow near stall points. International Gas Turbine and Aero engine Congress and Exposition, Orlando, ASME Paper No. 97-GT-88.

Rodgers, C., 1978. A diffusion factor correlation for centrifugal impeller stalling. J. Eng. Power, 100(4): 592-603.

Takayuki, H., M. Daisuke, O. Yutaka and O. Eisuke, 2011. Unsteady flow under surge and rotating stall in a three-stage axial flow compressor. J. Therm. Sci., 20(1): 6-12.

Vlad, H., F. Mohamed, R. Steven, B. Francisco and A. François, 2011. Experimental evidence of rotating stall in a pump-turbine at off-design conditions in generating mode. J. Fluids Eng., 133(5): 051104.

Wu, Y.H., Q.P. Li, W.L. Chu and H.G. Zhang, 2011. Unsteady flow mechanism of spike emergence in a subsonic axial flow compressor rotor. J. Northw. Polytech. Univ., 29(3): 491-495.